Eurasian Journal of Physics and Functional Materials

2018, 2(3), 219-230

Metal-insulator transitions and nanoscale phase separation in various underdoped cuprates

S. Dzhumanov, U.T. Kurbanov

Institute of Nuclear Physics, Uzbekistan Academy of Sciences, Tashkent, Uzbekistan

E-mail: dzhumanov@inp.uz

DOI: **10.29317/ejpfm.2018020303**
Received: 20.08.2018

We demonstrate that the unconventional electron-phonon interactions, charge inhomogeneity and charge ordering in underdoped cuprates play an important role in metal-insulator transitions and nanoscale phase separation. In so doing, we argue that charge carriers (i.e. hole polarons) in these systems segregate into insulating (carrier-poor) and metallic/superconducting (carrier-rich) regions as a result of their specific ordering. We show that the metal-insulator transitions, nanoscale phase separation and coexisting insulating and metallic/superconducting phases are manifested in the unusual temperature dependences of the magnetic susceptibility and resistivity and in the suppression of superconductivity in various underdoped cuprates.

Keywords: underdoped cuprate superconductors, phase separation, magnetic susceptibility, c-axis charge transport.

Introduction

The possible mechanisms of metal-insulator transitions and nanoscale phase separation in various classes of solids, including the doped copper-oxide (cuprate) high-T_c superconductors remain still unsolved problems in condensed matter physics [1-3]. The study of this problem is becoming increasingly important in connection with the need to solve such very important tasks as the obtaining of new promising dielectric, metallic and superconducting materials for the development of power engineering and microelectronics. Studies of high-T_c cuprate superconductors have shown that they exhibit various anomalous behaviors and

their electronic properties vary greatly with the change of the doping [1,3]. In particular, lightly doped cuprates exhibit unusual dielectric behaviors. With further increasing the doping level, cuprate compounds become unusual metals whose behavior is very different from behavior ordinary metals. High-T_c superconductivity in these materials appears in underdoped and optimally doped regimes. Namely, underdoped and optimally doped cuprates combine the most interesting insulating, metallic and SC properties that cannot be explained within the existing theories of insulators, metals and superconductors based on the standard band models of Wilson and Mott-Hubbard [1,4] and on the Bardeen-Cooper-Schrieffer (BCS) model of superconductivity [5]. Many attempts have been made to describe the unusual electronic properties of high-T_c cuprates within the framework of various theoretical models. Many of these approaches are based on the Hubbard-like models and on the so-called *t-J* models (see Refs.[1,3] for citation of initial literature sources), which describe strong electron correlations characterizing only undoped cuprates and ignore the effects of three-dimensionality of high-T_c materials and the most important electron-phonon interactions (i.e, polaron effects) inherent in doped polar materials. These approaches often lead to results that contradict each other, and therefore there are doubts about their adequacy and applicability even to underdoped cuprates [6]. The observed anomalies in the electronic properties of underdoped and optimally doped cuprates are believed to be closely related to the metal-insulator transitions, the phase separation and the coexistence of metal and insulating phases in these high-T_c materials, where the metal-insulator transitions are often observed in underdoped and even optimally doped systems and are characterized by a transition to the insulating behavior of the resistance at low temperature [7,8]. Metal-insulator transitions in doped cuprates are also manifested in the temperature dependence of their magnetic susceptibility χ. As follows from the above, for understanding the new electronic properties of doped high-T_c materials, it is first of all necessary to clarify the mechanisms of metal-insulator transitions and phase separation and to determine the possibility of the coexistence of metallic and insulating phases in underdoped regimes. So far, the relevant mechanisms of metal-insulator transitions and phase separation in doped cuprates have not been established exactly. Therefore, the solution of the problems of metal-insulator transitions and phase separation, as well as the determination of the nature of different anomalies in magnetic susceptibility and resistivity of underdoped high-T_c materials, require new theoretical approaches going beyond the existing standard theories of insulators and metals that have proved inadequate for these systems. In the present work we study the metal-insulator transitions and nanoscale phase separation and their manifestations in magnetic susceptibility and resistivity of various underdoped cuprates.

Relevant charge carriers and their ordering in doped cuprates

Upon p-type doping (hole doping) of the cuprates, the free holes introduced into the oxygen valence band interact with lattice vibrations and they become self-trapped quasiparticles (polarons) in a deformable lattice. A large ionicity of the cuprates $\eta = \varepsilon_\infty/\varepsilon_0 << 1$ (where ε_∞ and ε_0 are high-frequency and static dielectric constants, respectively) enhances the polar electron-phonon interaction and the tendency to polaron formation [9,10]. Actually, self-trapping of holes by now has been discovered in different classes of substances (including alkali halides [11,12] and cuprates [2,13]). Here we notice that the quasi-free electrons or holes can exist only in ordinary metals, monoatomic semiconductors (e.g. Si and Ge) and heavily overdoped cuprates.

Theoretical [9,10,14,15] and experimental [2,13,16] studies show that the charge carriers in doped cuprates are polarons with effective masses $m_p \simeq (2-3)m_e$ [2,17,18], where m_e is the free electron mass.

The underdoped cuprates are inhmogeneous systems (where the dopants and charge carriers are distributed inhomogeneously) and they are more inhomogeneous than overdoped cuprates [19]. One can assume that charge carriers (i.e., hole polarons) in these systems segregate into carrier-rich and carrier-poor regions as a result of their specific ordering. We argue that the charge ordering in carrier-poor and carrier-rich domains just like the ordering of atoms in solids, results in the formation of simple cubic, body-centered cubic and face-centered cubic superlattices with coordination numbers $z = 6, 8$ and 12, respectively, and the formation of different energy bands of polarons in the charge- transfer (CT) gap of the cuprates. In carrier-poor regions, a narrow polaronic band is formed inside the CT gap. In this case the system becomes an insulator where polaronic carriers become more localized and their hopping conductivity occurs within the narrow polaronic band. In contrast, the charge transport in sufficiently broadened polaronic band (i.e. in carrier-rich regions) becomes metal-like.

Metal-insulator transitions and phase separation in underdoped cuprates

As the doping increases towards underdoped region, specific charge ordering and segregation lead to the formation of dynamic (metallic) and static (insulating) stripes in carrier-rich and carrier-poor regions, where distinctly different superlattices of polarons are formed at their inhomogeneous spatial distribution. When the carrier-poor and carrier-rich regions coexist in underdoped cuprates, an important question arises: how and at what doping level $n = n_c$ the width of the polaronic band reaches a critical value above which polaron transport becomes metallic and a doped cuprate material can undergo a phase transition from an insulator to a metallic state? The criterion for such a metal-insulator transition can be written in the form [20]

$$\frac{E_p}{\varepsilon_F} \gtrsim 0.5\frac{a}{R_p}, \tag{1}$$

where a is the lattice constant of large polarons, R_p is the radius of such a polaron, $\varepsilon_F = \hbar^2(3\pi^2 n)^{2/3}/2m_p$ is the Fermi energy of large polarons.

The criterion (1) for a certain level of doping $n = n_c$ (where n is the density of polaronic carriers) can be rewritten as

$$x = x_c = \frac{n_c}{n_a} = \frac{1}{3\pi^2 n_a}\left[\frac{4m_p E_p R_p}{\hbar^2 a}\right]^{3/2}, \tag{2}$$

where $n_a = 1/V_a$ is the density of the host lattice atoms, V_a is the volume per CuO_2 formula unit in the cuprates.

For simple cubic, body-centered cubic and face-centered cubic superlattices of polarons with $z = 6$, $z = 8$ and $z = 12$, the lattice constants of non-overlapping polarons can be determined as $a = 2R_p$ (for $z = 6$), $a = (4/\sqrt{3})R_p$ (for $z = 8$) and $a = 2\sqrt{2}R_p$ (for $z = 12$). The minimum and maximum values of x_c determined from the relation (2) correspond to simple cubic and face-centered cubic superlattices of polarons. Therefore, applying the criterion (2) for metal-insulator transitions, in the cases of simple cubic and face-centered cubic polaron superlattices, we can write

$$x_{c1} = \frac{1}{3\pi^2\hbar^3 n_a}[2m_p E_p]^{3/2} \tag{3}$$

and

$$x_{c2} = \frac{1}{3\pi^2\hbar^3 n_a}[\sqrt{2}m_p E_p]^{3/2} \tag{4}$$

Now we estimate x_{c1} and x_{c2} for $La_{1-x}Sr_xCuO_4$ (LSCO) and $YBa_2Cu_3O_{7-\delta}$ (YBCO) by taking $m_p = (2.1 \div 2.7)m_e$ in LSCO [2,17,18] and $m_p = (2.0 \div 4.0)m_e$ in YBCO [2,21]. In so doing, we use the theoretical values of $E_p \simeq (0.09 \div 0.106)$ eV at $\varepsilon_\infty = 3.5$ and $\eta = 0.02 \div 0.10$ [20]. The values of V_a are determined approximately as follows. The lattice constants of the orthorhombic LSCO can be taken approximately $a = b \simeq 5.4$ and $c \simeq 13$ [22]. Then the volume of the primitive unit cell of LSCO is about 380 , while the volume per CuO_2 formula unit V_a in LSCO is equal to 190 . Further the lattice constants of $YBa_2Cu_3O_{7-\delta}$ are taken approximately $a = b \approx 4$ and $c \approx 12$ [22], so that the volume per CuO_2 formula unit in YBCO can be taken approximately $V_a \simeq 100$. Then, we find $n_a \simeq 0.53 \cdot 10^{22} cm^{-3}$ (for LSCO) and $n_a \simeq 10^{22} cm^{-3}$ (for YBCO). Using the above theoretical and experimental values of parameter m_p , E_p and n_a , we obtain the following values of critical dopings $x_{c1} \simeq 0.07 \div 0.131$ and $x_{c2} \simeq 0.042 \div 0.078$ for LSCO and $x_{c1} \simeq 0.035 \div 0.125$ and $x_{c2} \simeq 0.021 \div 0.074$ for YBCO. We see that in underdoped LSCO, the metal-insulator transitions and phase separation into carrier-rich metallic (at $x > x_{c1}$ and $x > x_{c2}$) regions and carrier-poor insulating (at $x < x_{c2}$ and $x < x_{c1}$) regions may occur in the doping range from $x \simeq 0.042$ (lightly doped region) to $x \gtrsim 0.131$ (moderately underdoped

region including also the "magic doping $x = 1/8$"), while such metal-insulator transitions and phase separation in underdoped YBCO would occur in the doping range from $x \simeq 0.021$ to $x \simeq 0.125$. These results are in reasonable agreement with experimental data on metal-to-insulator crossover and stripe formation in underdoped cuprates [23-26]. In particular, the above results provide a natural explanation for the so-called $1/8$ anomaly in the underdoped cuprates. According to our results, the doping level $x = 1/8$ is of vital importance for various underdoped cuprates, since the part of dynamic stripes becomes static at $x \leq 1/8$ and metallic/superconducting domains begin decreasing just at this doping level. In the experiment the total resulting effects of the different coexisting (simple-cubic and face-centered cubic) superlattices of charge carriers are manifested but the effect of each of these superlattices is not manifested separately.

Possible manifestations of the metal-insulator transitions and phase separation in underdoped cuprates

Attempts to explain the unusual normal-state properties of underdoped cuprates (in particular, insulator-metal crossover taking place far in the superconducting region, the insulating behavior of the c-axis resistivity and the temperature-dependent magnetic susceptibility in the metallic state) and their suppressed superconductivity (hiding the normal-state properties) and pseudogap behaviors have led to many controversial assumptions (see, e.g., Refs. [1,27,28]). Unconventional interactions between quasiparticles in underdoped cuprates may lead to their new and unidentified electronic states. In reality, the unconventional electron-phonon coupling and polaronic effects are major factors influencing the electronic properties (in particular, magnetic susceptibility and resistivity) of underdoped cuprates.

As is well known, the magnetic susceptibility and electric conductivity in the normal state of underdoped cuprates are different from the one explained by the usual band theory. Although, some researchers have started to construct the theory of the magnetic susceptibility and charge transport in the cuprates [27,29-32], the magnetic susceptibility and the charge transport in the c-direction have seldom been investigated. We now discuss the problem of the insulator-to-metal crossover by studying the doping and temperature dependences of the magnetic susceptibility and c-axis resistivity of underdoped cuprates. In so doing, we use the large bipolaron model, the impurity and polaron band models, which are valid in the bulk. We also use the unusual form of BCS-like pairing theory of polarons and believe that such a modified BCS-like theory is applicable in the bulk of the underdoped cuprates. In the following, we study the possible manifestations of the metal-insulator transitions and coexisting insulating and metallic/superconducting phases in the temperature dependences of the magnetic susceptibility $\chi(T)$ and the c-axis resistivity $\rho_c(T)$ of the underdoped cuprates within the pertinent theoretical approaches taking into account the real physical situation in these systems. In the lightly doped cuprates ($x \lesssim 0.05$), both defect centers and polarons (which are products of the thermal dissociation of large

bipolarons residing between the CuO_2 layers) contribute to $\chi(T)$. In this case the $\chi(T)$ can be determined from the relation

$$\chi(T) = \chi_D(T) + \chi_p^*(T) = \frac{\mu_B^2}{k_B T} n_D - 2\mu_B^2 \int_0^\infty D_p(\varepsilon) \frac{\partial f_p^*}{\partial \varepsilon} d\varepsilon, \tag{5}$$

where $\chi_D(T)$ and $\chi_p^*(T)$ are the contributions to $\chi(T)$ coming from defect centers and polaronic carriers, respectively, $f_p^*(\varepsilon) = [exp((\varepsilon + E_{bB})/k_B T) + 1]^{-1}$ is the Fermi distribution function for the polarons produced by thermal dissociation of bipolarons, E_{bB} is the binding energy of a large bipolaron, $D_p(\varepsilon) = (\sqrt{2} m_p^{3/2}/\pi^2\hbar^3)\sqrt{\varepsilon}$ is the density of states of polarons, μ_B is the Bohr magneton, n_D is the density of defect centers.

The first term in Eq.(5) is nothing other than the Curie law $\chi_D(T) \sim 1/T$ for localized carriers, while contribution of thermally dissociated bipolarons to $\chi(T)$ is

$$\chi_p^*(T) = \frac{2\sqrt{2}\mu_B^2 m_p^{3/2}\sqrt{k_B T}}{\pi^2\hbar^3} \times e^{E_{bB}/k_B T} \int_0^\infty \frac{\sqrt{y} e^y}{(e^{(E_{bB}/k_B T)} e^y + 1)^2} dy, \tag{6}$$

where $y = \varepsilon/k_B T$.

The variation of $\chi(T)$ in the lightly doped cuprate LSCO is shown in Fig.1. As can be seen by inspection of Fig.1, $\chi(T)$ decreases with decreasing temperature, reaches a minimum, and then increases exhibiting an insulating behavior, in agreement with experimental $\chi(T)$ curve for the lightly doped LSCO ($x = 0.05$) [33]. In Fig.1, our theoretical curve is a much best fit of the experimental points and the expression (5) describes fairly well the insulating behavior of the magnetic susceptibility $\chi(T)$.

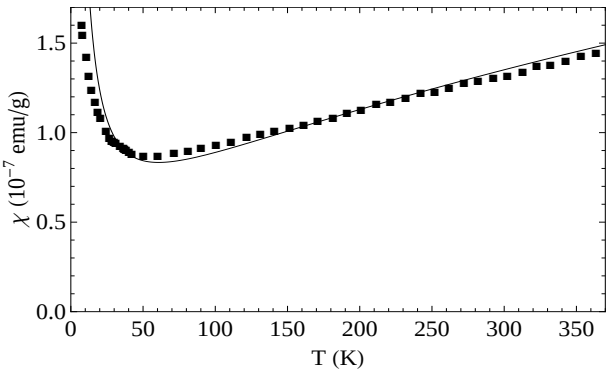

Figure 1. Temperature dependence of χ in the lightly doped cuprate $La_{2-x}Sr_xCuO_4$ (x =0.05) with parameters $m_p = 4.3m_e$, $n_D = 0.145 \cdot 10^{20} cm^{-3}$, $\rho_M = 4.2 g/cm^3$, and $E_{bB} = 0.0018$ eV. The theoretical results (solid curve) are compared with experimental data (■) [33].

When the density of impurity (dopant) centers and polarons increases, the impurity and polaronic states form energy bands in which the charge transport becomes band-like (i.e. metal-like). We argue that Cooper pairing of polarons at a characteristic temperature T^* above T_c may occur in a degenerate polaronic Fermi gas with $\varepsilon_F >> k_B T$, namely, in sufficiently broadened polaronic band

[34], while the charge carriers in the impurity band (i.e., charge carriers trapped by impurities) remain unpaired [35].

Therefore, large bipolarons and polaronic Cooper pairs as the bound pairs of fermions are dissociated into two separate polarons with increasing the temperature. In underdoped and nearly optimally doped cuprates, defect centers, unpaired charge carriers in the impurity band, thermally dissociated large bipolarons and polaronic Cooper pairs contribute to $\chi(T)$. Thus, the expression for $\chi(T)$ in underdoped and nearly optimally doped cuprates can be written as

$$\chi(T) = \chi_D(T) + \chi_I(T) + \chi_p^*(T) + \chi_C(T), \tag{7}$$

where

$$\chi_I(T) = -2\mu_B^2 \int_0^\infty D_I(\varepsilon) \frac{\partial f_I(\varepsilon)}{\partial \varepsilon} d\varepsilon \tag{8}$$

is the contribution to $\chi(T)$ coming from the charge carriers in the impurity band, $D_I(\varepsilon) = (\sqrt{2} m_I^{3/2} / \pi^2 \hbar^3) \sqrt{\varepsilon}$ is the density of states in the impurity band, $f_I(\varepsilon) = [exp((\varepsilon - \varepsilon_{FI})/k_B T) + 1]^{-1}$ is the Fermi distribution function for the carriers in the impurity band (where the energy ε of carriers is measured from the Fermi energy ε_{FI}) and m_I are the mass of carriers in this band,

$$\chi_C(T) = -2\mu_B^2 \int_0^\infty D_c(\varepsilon) \frac{\partial f_c(\varepsilon)}{\partial \varepsilon} d\varepsilon \tag{9}$$

is the contribution to $\chi(T)$ coming from the polaronic components of the thermally dissociated Cooper pairs, $D_c(\varepsilon) = D_p(\varepsilon)/2$ is the density of states at the Fermi surface for polarons of one spin orientation introduced in the BCS pairing theory [3], $f_c(\varepsilon) = \left[exp(\sqrt{\varepsilon^2 + \Delta^{*2}(T)}/k_B T) + 1\right]^{-1}$ is the Fermi distribution function for the excited polaron components of Cooper pairs, $\Delta^*(T)$ is a BCS-like energy gap (or pseudogap) in the excitation spectrum of polaronic Cooper pairs, which can be approximated by the following more simple analytical expression

$$\Delta^*(T) \simeq 1.76 k_B T^* \tanh\left[1.85\sqrt{\frac{T^*}{T} - 1}\right]. \tag{10}$$

One can assume that the main contribution both to $\chi_C(T)$ and to BCS-like pairing of polarons below T^* comes from polaronic carriers whose energy is close to the Fermi energy ε_F. Then, $D_c(\varepsilon)$ in Eq.(9) can be replaced by $D_c(\varepsilon_F)$. As a result, we obtain

$$\chi_C(T) \simeq 2\mu_B^2 D_c(\varepsilon_F)[1 + exp(\Delta^*(T)/k_B T)]^{-1} \tag{11}$$

The final expression for $\chi(T)$ is

$$\chi(T) \simeq \mu_B^2 \left\{ \frac{n_D}{k_B T} + \frac{2\sqrt{2} m_I^{3/2}}{\pi^2 \hbar^3 k_B T} \int_{\varepsilon_{FI}}^{\infty} \sqrt{\varepsilon} \frac{e^{(\varepsilon-\varepsilon_{FI})/k_B T}}{[e^{(\varepsilon-\varepsilon_{FI})/k_B T}+1]^2} d\varepsilon + \right.$$
$$+ \frac{2\sqrt{2} m_p^{3/2}}{\pi^2 \hbar^3 k_B T} \int_{0}^{\infty} \sqrt{\varepsilon} \frac{e^{(\varepsilon+E_{bB})/k_B T}}{[e^{(\varepsilon+E_{bB})/k_B T}+1]^2} d\varepsilon +$$
$$\left. + \frac{2 m_p^{3/2}}{\sqrt{2}\pi^2 \hbar^3} \frac{1}{(1+e^{\Delta^*(T)/k_B T})} \sqrt{\varepsilon_F} \right\}. \qquad (12)$$

In the normal state of underdoped and optimally doped cuprates, a BCS-like pseudogap $\Delta^*(T)$ is manifested in $\chi(T)$ below T^* as shown in Fig.2 for the underdoped $YBa_2Cu_3O_{6+x}$. At high temperatures $T >> T^*$ the magnetic susceptibility of these high-T_c cuprates depends weakly on temperature. According to (12), $\chi(T)$ begins to decrease gradually with lowering the temperature down to T^* and then the decrease in $\chi(T)$ with lowering T below T^* becomes more rapid (see Fig.2) due to the appearance of the pseudogap Δ^* in the excitation spectrum of the underdoped $YBa_2Cu_3O_{6+x}$ for which we took the mass density $\rho_M = 6.4 g/cm^3$ and molar mass $M = 670 g/mole$ [36] in our calculations.

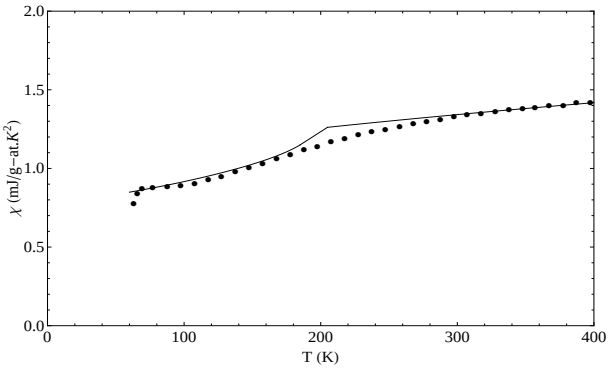

Figure 2. Comparison of the theoretical results for the magnetic susceptibility of the high-T_c cuprate $YBa_2Cu_3O_{6+x}$ (solid curve obtained using the parameters $m_p = 2.35 m_e$, $m_I = 3.3 m_e$, $n_D = 0.05 \cdot 10^{19} cm^{-3}$, ε_F =0.127 eV, ε_{FI} =0.087 eV, E_{bB} =0.0006 eV) with experimental data for x =0.62 (•) [37].

In ordinary metals, $\chi(T)$ is temperature independent due to absence of a polaronic effect. In contrast, a polaronic signature appears in $\chi(T)$ both above T^* and below T^* in underdoped cuprtaes where $\chi(T)$ first begins to decrease slowly with lowering the temperature down to T^* and then the decrease in $\chi(T)$ with lowering T below T^* becomes more rapid (see Fig.2).

We now consider optimally doped YBCO, where the binding energy E_{bB} of bipolarons residing between the CuO_2 layers becomes vanishingly small and the temperature T^* is very close to T_c. Here the defect centers, charge carriers in the broadened impurity band (where $\varepsilon_{FI} >> k_B T$), thermally dissociated large bipolarons and polaron components of dissociated Cooper pairs contribute to the magnetic susceptibility of these high-T_c materials and the full expression for $\chi(T)$ can be written as

$$\chi(T) = \chi_D(T) + \chi_I(T) + \chi_p^*(T) + \chi_C(T) = \mu_B^2 \left\{ \frac{n_D}{k_B T} + \right.$$
$$+ \frac{2\sqrt{2} m_I^{3/2}}{\pi^2 \hbar^3 k_B T} \sqrt{\varepsilon_{FI}} + \frac{2\sqrt{2} m_p^{3/2}}{\pi^2 \hbar^3 k_B T} \int_0^\infty \sqrt{\varepsilon} \frac{e^{(\varepsilon + E_{bB})/k_B T}}{[e^{(\varepsilon + E_{bB})/k_B T} + 1]^2} d\varepsilon +$$
$$\left. + \frac{2 m_p^{3/2}}{\sqrt{2} \pi^2 \hbar^3} \frac{1}{(1 + e^{\Delta^*(T)/k_B T})} \sqrt{\varepsilon_F} \right\}. \qquad (13)$$

In this case, the magnetic susceptibility $\chi(T)$ calculated according to (13) is weakly temperature-independent (see Fig.3), as observed also experimentally in the optimally doped YBCO [37]. From the above considerations, it follows that the coexisting insulating and metallic phases are manifested in the temperature dependence of the magnetic susceptibility χ of underdoped to optimally doped cuprates.

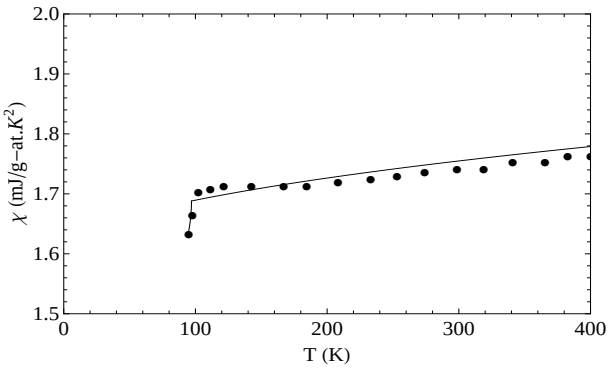

Figure 3.Comparison of the theoretical results for the magnetic susceptibility of the high- T_c cuprate $YBa_2Cu_3O_{6+x}$ (solid curve obtained using the parameters $m_p = 1.7m_e$, $m_I = 2.7m_e$, $n_D = 0.01 \cdot 10^{19} cm^{-3}$, ε_F =0.21 eV, and ε_{FI} =0.148 eV) with experimental data for x =0.97 (•) [37].

Further, the analysis of the c-axis charge transport in high- T_c cuprates at different doping levels may also provide additional information on the insulating and metallic behaviors of these materials. The transport mechanisms in and out of plane are actually different. Here we consider specifically 3D polaron transport at the dissociation of interlayer large bipolarons for studying the problem of insulator- to-metal crossover in the bulk of the cuprates. We assume that in doped cuprates the localized large bipolarons are formed in carrier-poor regions between the CuO_2 layers and the c-axis charge transport becomes possible at the thermal dissociation of these immobile bipolarons into the separate polarons which subsequently move by hopping along the c-axis. According to Ref.[31], the c-axis resistivity of the cuprates above T_c can be determined as

$$\rho_c(T) = \rho_0 + \frac{2 k_B T}{n_i e^2 a_h^2 \omega_0} exp \left[\frac{E_{bB}}{k_B T} \right], \qquad (14)$$

where ρ_0 is the residual resistivity, a_h is the hopping distance, ω_0 is the out-of-plane optical phonon mode frequency.

Now, we will compare our predictions with the experimental $\rho_c(T)$ data for $YBa_2Cu_3O_y$ at various doping levels. In so doing,we apply the model based on the hopping conduction of polarons at thermally activated dissociation of localized bipolarons residing between the CuO_2 layers to the c-axis charge transport observed in $YBa_2Cu_3O_y$. Comparison of our results with experimental $\rho_c(T)$ data for various samples of $YBa_2Cu_3O_y$ with different doping levels is shown in Fig.4. One can see that the calculated results for $\rho_c(T)$ agree very well with the experimental $\rho_c(T)$ data down to T_c. As can be seen by inspection of Fig.4, the insulating behavior of $\rho_c(T)$ in underdoped $YBa_2Cu_3O_y$ is charged gradually to the metallic behavior with decreasing E_{bB} in optimally doped regime, as shown in Fig.4.

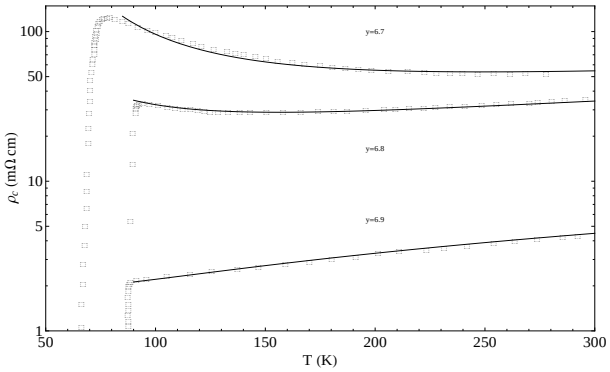

Figure 4. The experimental $\rho_c(T)$ data (dotted square) obtained for $YBa_2Cu_3O_y$ at various doping levels [38] and the respective fits using Eq.14 (solid lines). Fits to the experimental $\rho_c(T)$ data for $YBa_2Cu_3O_y$ with $y = 6.7$, 6.8 and 6.9 are performed using Eq.14 and different fitting parameters (i.e., the following fitting parameters $\rho_0 = 0.05m\Omega cm$, $a_h = 11.5 \cdot 10^{-8} cm$, $\omega_0 = 5.8 \cdot 10^{13} s^{-1}$, $n_i = 1.77 \cdot 10^{19} cm^{-3}$, $E_{bB} = 0.0215$ eV; $\rho_0 = 0.03m\Omega cm$, $a_h = 11.5 \cdot 10^{-8} cm$, $\omega_0 = 6.0 \cdot 10^{13} s^{-1}$, $n_i = 2.0 \cdot 10^{19} cm^{-3}$, $E_{bB} = 0.0135$ eV and $\rho_0 = 0.02m\Omega cm$, $a_h = 11.5 \cdot 10^{-8} cm$, $\omega_0 = 17.0 \cdot 10^{13} s^{-1}$, $n_i = 7.35 \cdot 10^{19} cm^{-3}$, $E_{bB} = 0.005$ eV are used for y = 6.7, 6.8 and 6.9, respectively.

Conclusion

We have studied the metal-insulator transitions and nanoscale phase separation and their possible manifestations in various unusual behaviors of underdoped high-T_c cuprates. We argued that charge carriers introduced into cuprates by hole doping become polaronic quasiparticles and segregate into insulating (carrier-poor) and metallic/superconducting (carrier-rich) regions as a result of their specific ordering. Our results show that the insulating and metallic phases coexist first in the lightly doped cuprates ($x \simeq 0.02 - 0.05$) and then the coexistence of the competing insulating, metallic and superconducting phases is expected in underdoped cuprates ($x \simeq 0.05 - 0.13$). The competition between coexisting insulating and metallic/superconducting phases rules the behavior of these materials. We demonstrated that the metal-insulator transitions and nanoscale phase separation are manifested in the unusual temperature-dependent behaviors of the magnetic susceptibility and resistivity and in the suppression of the critical superconducting transition temperature in various underdoped cuprates.

Acknowledgments

We thank E.M. Ibragimova, P.J. Baimatov and E.X. Karimbaev for useful discussions. This work was supported by the Foundation of Uzbekistan Academy of Sciences, grant No. OT-Ф2-15.

References

[1] M. Imada et al., Rev. Mod. Phys. **70** (1998) 1039 .
[2] M.A. Kastner et al., Rev. Mod. Phys. **70** (1998) 897.
[3] S. Dzhumanov, Theory of Conventional and Unconventional Superconductivity in the High-T_c Cuprates and Other Systems (Nova Science Publishers, New York, 2013).
[4] F. Walz, J. Phys.: Condens. Matter **14** (2002) R285.
[5] J. Bardeen et al., Phys. Rev. **108** (1957) 1175.
[6] V.I. Belyavsky et al., UFN **175** (2005) 191.
[7] S. Ono et al., Physica C **357?60** (2001) 138.
[8] G.S. Boebinger et al., Phys. Rev. Lett. **77** (1996) 5417.
[9] D. Emin, M.S. Hillery, Phys. Rev. B **39** (1989) 6575.
[10] J.T. Devrees, A.S. Alexandrov, Rep. Prog. Phys. **72** (2009) 066501.
[11] Ch.B. Lushchik, A. Ch. Lushchik, Decay of electronic excitations with defect formation in solids (Nauka, Moscow, 1989).
[12] S. Dzhumanov, P.K. Khabibullaev, Phys. Stat. Sol. B **152** (1989) 395.
[13] S. Sugai, Physica C **185-189** (1991) 76.
[14] G. Verbist et al., Phys. Scripta T **39** (1991) 66.
[15] S. Dzhumanov et al., Physica C **254** (1995) 311.
[16] X.X. Bi, P.C. Eklund, Phys. Rev. Lett. **70** (1993) 2625.
[17] A. Ino et al., Phys. Rev. B **65** (2002) 094504.
[18] D.N. Basov, T. Timusk, Rev. Mod. Phys. **77** (2005) 721.
[19] T. Kato et al., Physica C **460-462** (2007) 880.
[20] S. Dzhumanov et al., J. Phys. Chem. Solids **73** (2012) 484.
[21] A.V. Puchkov et al., J. Phys:Condens. Matter **8** (1996) 10049.
[22] Yu.A. Izyumov et al., Usp. Fiz. Nauk. **159** (1989) 621.
[23] Sh. Sakita et al., J. Phys. Soc. Jpn. **68** (1999) 2755.
[24] Y. Koike et al., Physica C **357-360** (2001) 82.
[25] J. Fink et al., Physica C **185-189** (1991) 45.
[26] S. Ono et al., Physica C **357-360** (2001) 138.
[27] A.A. Abrikosov, Phys. Usp. **41** (1998) 605.
[28] S.I. Vedeneev, Phys. Usp. **182** (2003) 669.
[29] D. Pines, Tr. J. Phys. **20** (1996) 535.
[30] B.P. Stojkovic, D. Pines, Phys. Rev. B**55** (1997) 8576.
[31] S. Dzhumanov et al., Physica B **440** (2014) 17.
[32] P.W. Anderson, The theory of superconductivity in the high-T_c cuprates (Prinston Univ. Press, Prinston, 1997).
[33] T. Nakano et al., Phys. Rev. B **49** (1994) 16000.

[34] S. Dzhumanov et al., Phys. Lett. A **380** (2016) 2173.
[35] S. Dzhumanov, E.K. Karimbaev, Physica A **406** (2014) 176.
[36] M. Roulin et al., In Physics and Materials Science of Vortex States, Flux Pinning and Dynamics, Edited by: R. Kossowsky, S. Bose, Z. Durusoy, V. Pan (Springer, New York, 1999) 489.
[37] J.W. Loram et al., Physica C **235-240** (1994) 134.
[38] S. Tajima et al., Phys. Rev. B **55** (1997) 6051.